Compact Stellarator Coils

N. Pomphrey[1], L. Berry[2], A. Boozer[3],
A. Brooks[1], R. Hatcher[1], S. Hirshman[2],
L-P. Ku[1], W. Miner[4], H. Mynick[1],
W. Reiersen[1], D. Strickler[2], P. Valanju[4]

[1] Princeton Plasma Physics Laboratory, Princeton, NJ 08543, USA
[2] Oak Ridge National Laboratory, Oak Ridge, TN 37831-8070, USA
[3] Columbia University, New York, NY 10027, USA
[4] University of Texas at Austin, Austin, TX 78712-1081, USA

Outline

We present a summary of several innovations made in the course of designing flexible coilsets for proposed compact stellarator experiments within the US fusion program. These may be useful in future stellarator design efforts. The innovations include:

1. Current Sheet Coil Improvements using SVD

2. Control Matrices for Sensitivity Analysis

3. Genetic Algorithm for Cutting Discrete Coils

4. Development of Alternate Coil Topologies

5. Fast Code for Designing Modular Coils

6. Integrated Coil-Plasma Design Methods

1. Current Sheets using SVD[1]

NESCOIL[2] is a key tool for stellarator coil design:

On a coil winding surface (CWS) NESCOIL $\Rightarrow$ sheet current $\vec{j}' = \hat{n}' \times \nabla\Phi(u,v)$. s.t. $b = \vec{B} \cdot \hat{n}$ vanishes on the plasma boundary. Fourier cpts of Φ are obtained by solving "Inductance Eqs' $\boxed{L\{\Phi_{mn}\} = \{b_{uv}\}. \quad (1)}$

Discrete coils are obtained by selecting appropriate contours of Φ and interpreting them as filamentary coils.

Ill-conditioning of Eq. (1) can result in large current densities and complex coil contours on the CWS, particularly if the CWS is well-separated from the plasma.

Using Singular Value Decomposition (SVD)[3] methods to solve Eq 1 results in smoother coil contours than standard NESCOIL. By varying the singular value cutoff, we can also exploit an important tradeoff between B-fitting error and coil current density, as seen in Fig. 1.

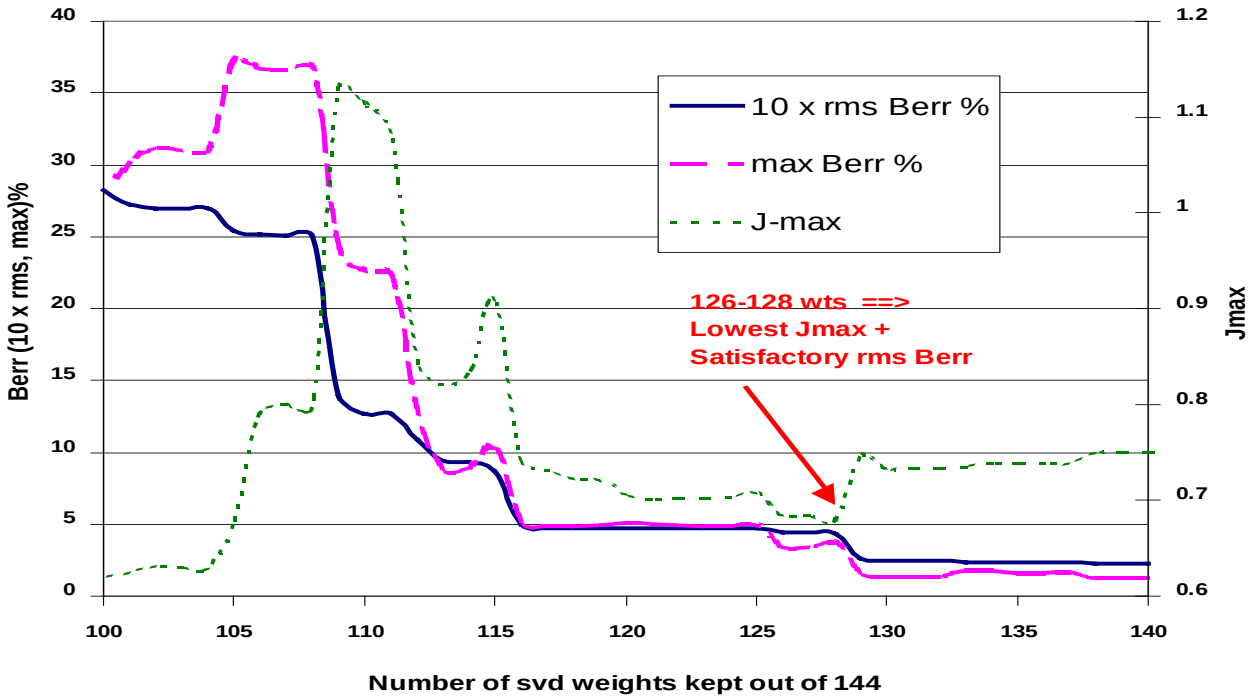

Figure 1: SVD Scan for LI383 Saddle Current Sheet showing trade-off between B-fitting error (B_{err}) and maximum current density (J_{max}). As the number of singular values is varied, a family of current sheet solutions is obtained. The r.m.s B_{err} should be $< 1\%$ to allow an accurate equilibrium reconstruction of the plasma. In some cases, reductions in current sheet density of up to 50% have been obtained compared with the standard NESCOIL least-squares solution.

2. Control Matrices[4]

The ability to control kink stability (KS) and quasi-axisymmetry (QA) are key elements of a compact stellarator experiment.

To determine which combination of coil currents can independently control the KS and QA, we should understand what plasma boundary shape changes control these important physics properties.

Control Matrices (CM's) provide this information:-

Let $\mathbf{Z}$ denote a set of N parameters that describe a plasma shape, and $\mathbf{P}$ a set of M physics properties that are to be controlled.

Expanding $\mathbf{P(Z = Z_0 + z) = P(Z_0) + p}$ about a particular configuration $\mathbf{Z_0}$ gives, to 1st order,

$$\mathbf{p = C_0 \cdot z.} \qquad (1)$$

$\mathbf{C_0 \equiv C(Z_0)}$ is the CM at design point Z_0.

After calculating $\mathbf{C_0}$ using VMEC and TERPSICHORE, this $M \times N$ matrix is inverted by SVD:

$$\mathbf{C_0 = U \cdot \Sigma \cdot V^T} \Rightarrow \boxed{\xi^{\mathbf{i}} = \mathbf{C_0^+} \cdot \pi^{\mathbf{i}} \quad (2),} \quad \text{with}$$

$\pi^{\mathbf{i=1,M}}$ unit base vectors in the $\mathbf{P}$ space.

The $\xi^{\mathbf{i}}$ are displacements which change a single physics parameter (e.g., kink growth rate or QA transport) leaving all others unchanged.

Fig. 2 shows a plot of the boundary shape changes which independently control the KS and QA for a particular NCSX configuration.

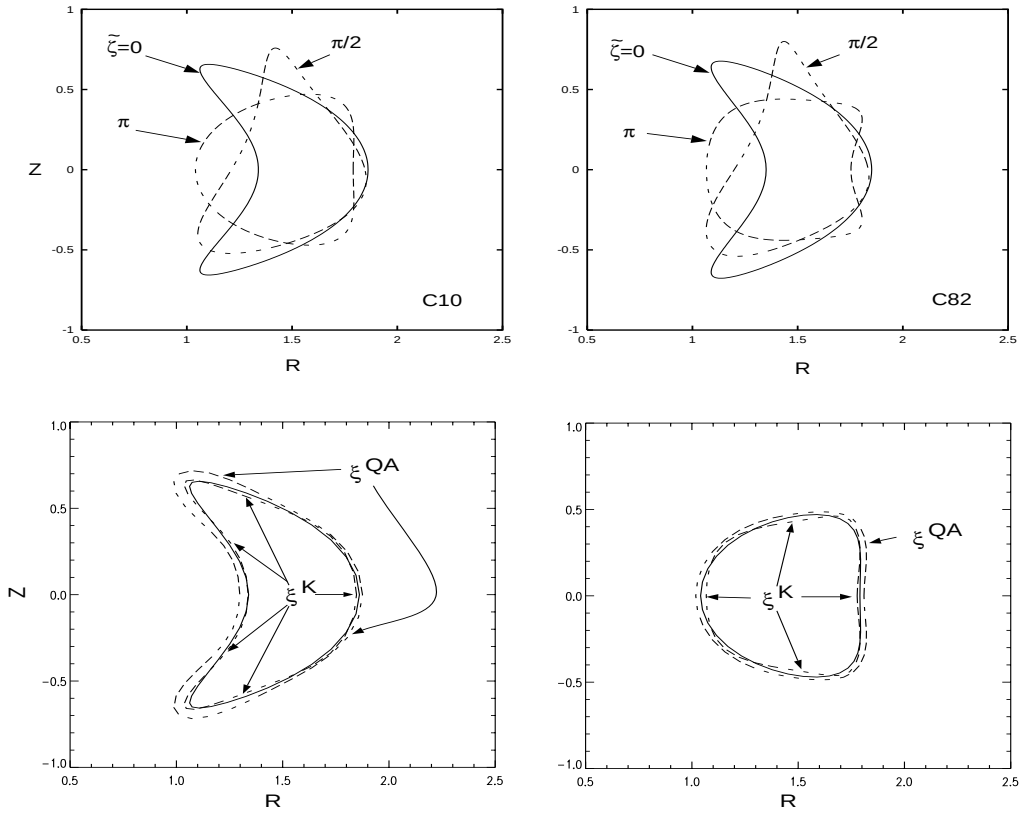

Figure 2: Top frames show poloidal cross sections of two NCSX plasma configurations. c82 is stable to external kinks at $\beta = 4\%$; c10 is unstable[5]. Bottom frames show ξ^i solutions of the CM Eq. (2). The ξ^i physically represent plasma boundary displacements which change a single physics parameter, such as the kink mode growth ($i = K$), or QA transport ($i = QA$), leaving the others unchanged. Note that the CM solution correctly associates increasing outboard indentation at the half-period symmetry plane with increasing kink stability.

Future Directions for CM applied to Coils:

The $N - M$ vectors $\mathbf{v^{i=M+1,\cdots,N}}$ formed out of those columns of $\mathbf{V}$ which are associated with singular values equal to zero span the "nullspace" of $\mathbf{C_0}$.
i.e., $\mathbf{C_0 \cdot v^i = 0}$.

In principle, one can use these $\mathbf{v^i}$ vectors to find alternative stellarator boundaries, having the same desirable physics properties, but improved engineering.

3. Genetic Algorithm for Discrete Coils[6]

Discrete coils can be obtained from a current sheet solution, $\Phi(u, v)$, by selecting N_c appropriate contours of Φ and interpreting each as a filamentary coil.

The question is, which set of N_c potential coils should be selected? We treat this as a global optimization problem subject to the following constraints:

(1) The number of coils should be small to allow for access and heating,

(2) Plasma reconstruction errors should be small enough ($b^{rms} < 1\%$) to reproduce the desired physics,

(3) The maximum coil current density should be small enough ($< 20 kA/cm^2$) to allow for an adequate flattop time.

A Genetic Algorithm[7] has been very successful in finding attractive solutions (see Figs 3-4).

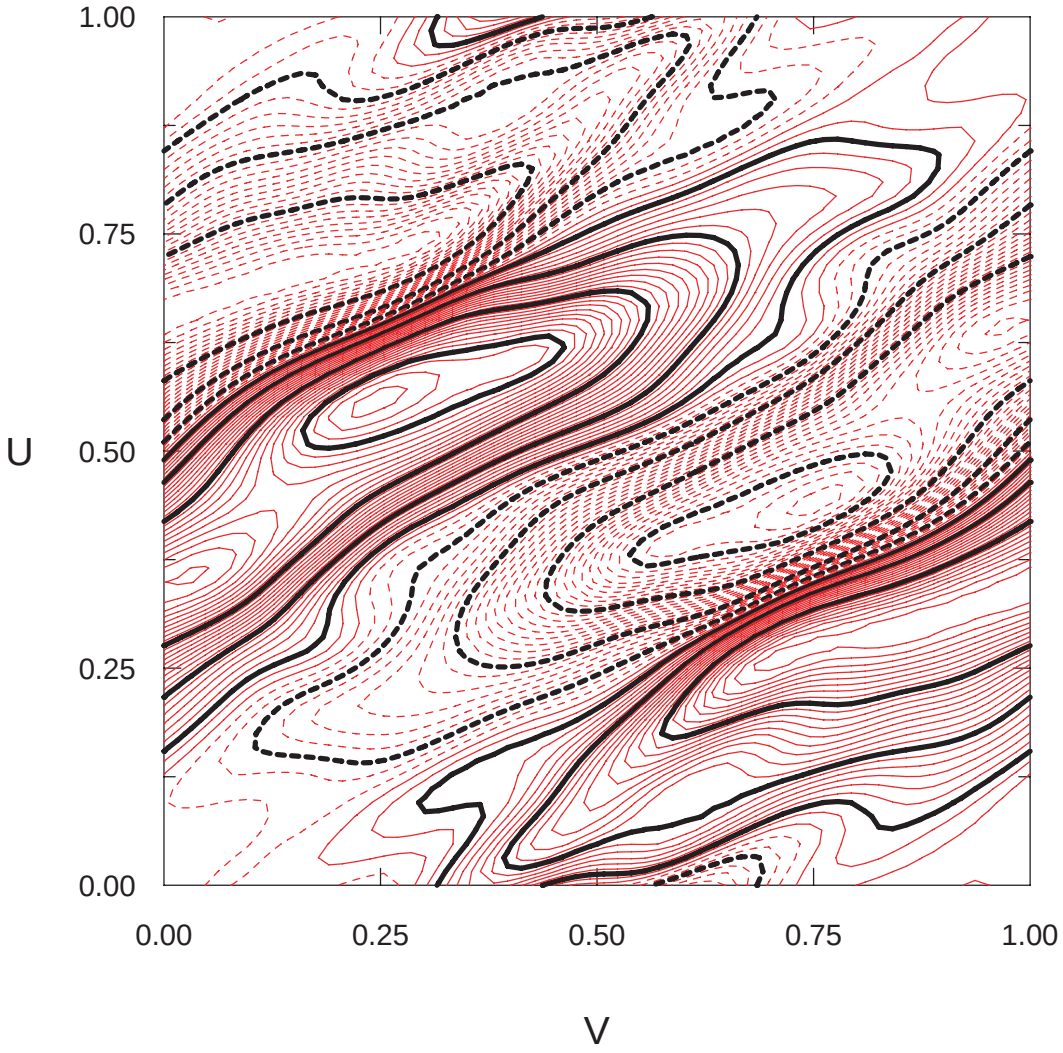

Figure 3: Sixty contours of the current potential (red) for configuration LI383 obtained by SVD. These form a pool of potential coils from which the GA must select a small number, N_c satisfying various physics and engineering constraints. An attractive solution with $N_c = 4$ (see also Table 1) is shown in black

Method	N_c	$B_{err}^{rms}\%$	$B_{err}^{max}\%$	$I_c^{max}[kA/cm^2]$
Equi-Φ	13	0.95	7.0	14.7
GA	7	0.52	2.8	14.2
GA	6	0.61	3.8	12.7
GA	5	0.77	5.7	13.2
GA	4	0.92	5.0	14.2

Table 1: Comparison of mean and max fitting errors at plasma boundary, and max coil current density, for various numbers of coils per half-period. The Genetic Algorithm has decreased the required number of coils in this NCSX saddle coil design from 13 to 4, preserving the physics and engineering constraints.

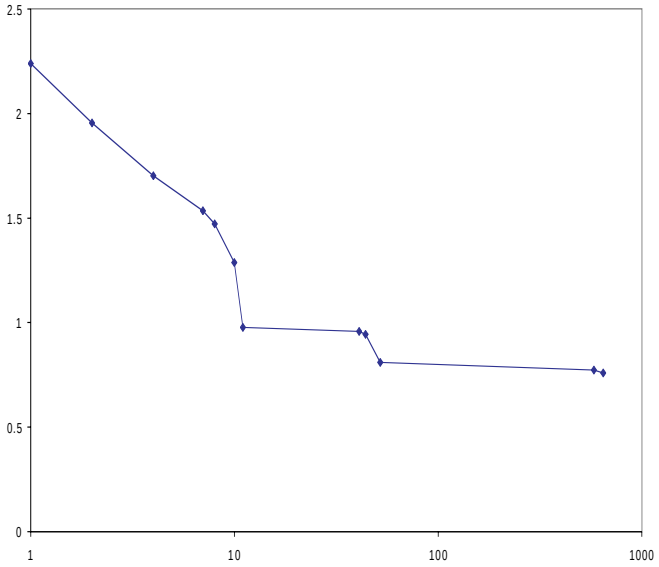

Figure 4: RMS fitting error, b^{rms}, obtained by the GA as a function of the number of generations for $N_c = 4$ coils per half-period, and applied to LI383.

4. Alternate Coil Topologies

Initial NCSX configurations were based on a saddle coil design that uses a 1/R TF field for providing toroidal flux (see Fig. 5) with saddle coils located in machined grooves on a monolithic shell surrounding the plasma.

To decrease engineering difficulties (high coil current densities, complex coil topology, limited access due to the TF coils and supports), alternate background coil topologies were explored to better understand the merits/demerits of the 1/R option by comparing it with the alternatives.

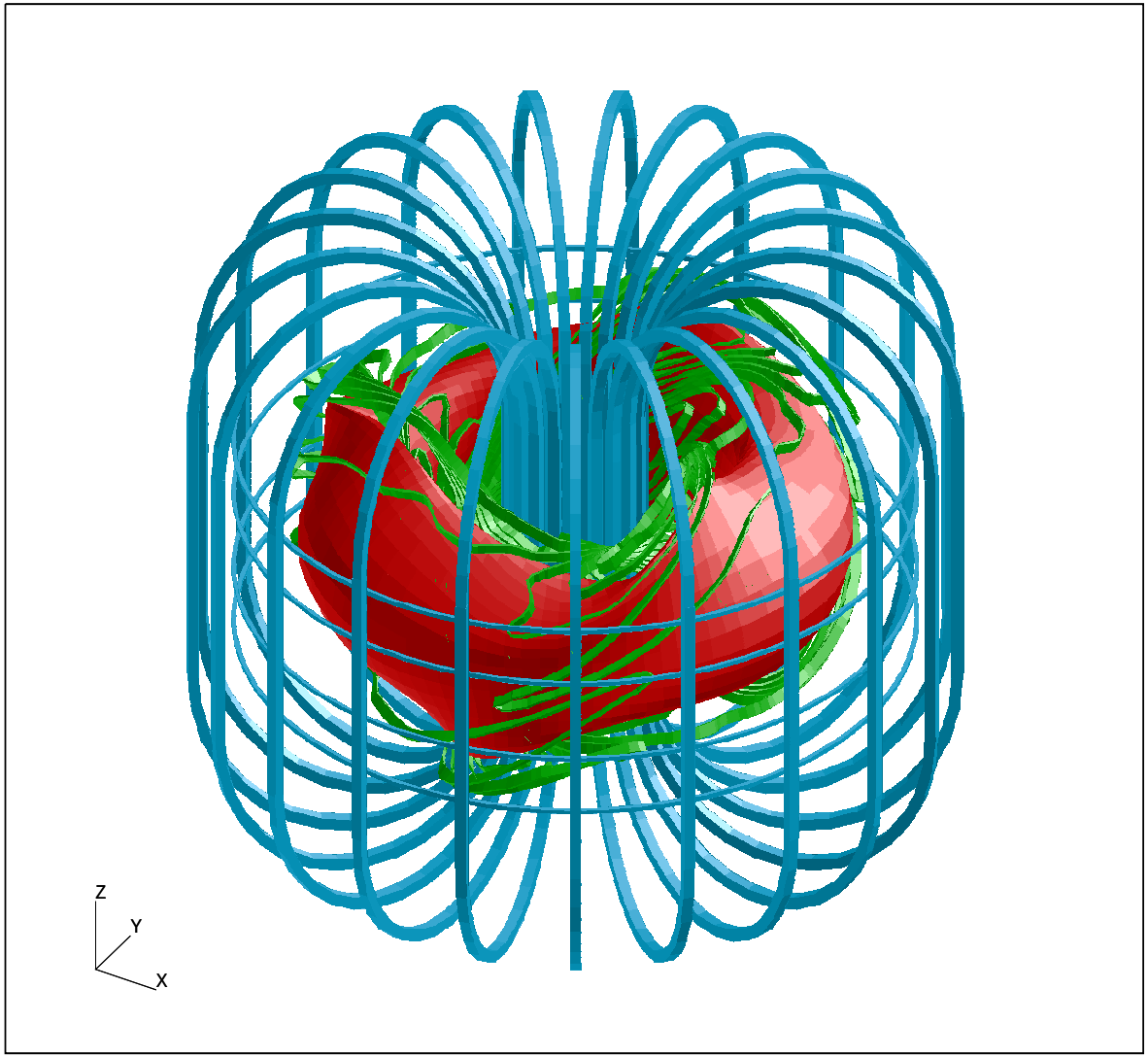

Figure 5: Saddle coil option based on using existing PBX TF and PF coils. Saddle coils are shown in green.

Background coilsets were obtained by optimizing the position, tilt angle, etc of fairly simple, constructable, coils which better "fit" the basic plasma shape.

The background coil design that was the most effective in reducing the current density of the saddle coils (by $> 60\%$) is shown in Fig. 6, featuring 3 circular tilted, interlocking coils that enclose the major axis and the plasma (L=3 coils), 3 circular (vertical) TF coils, and 1 pair of circular PF coils for equilibrium control.

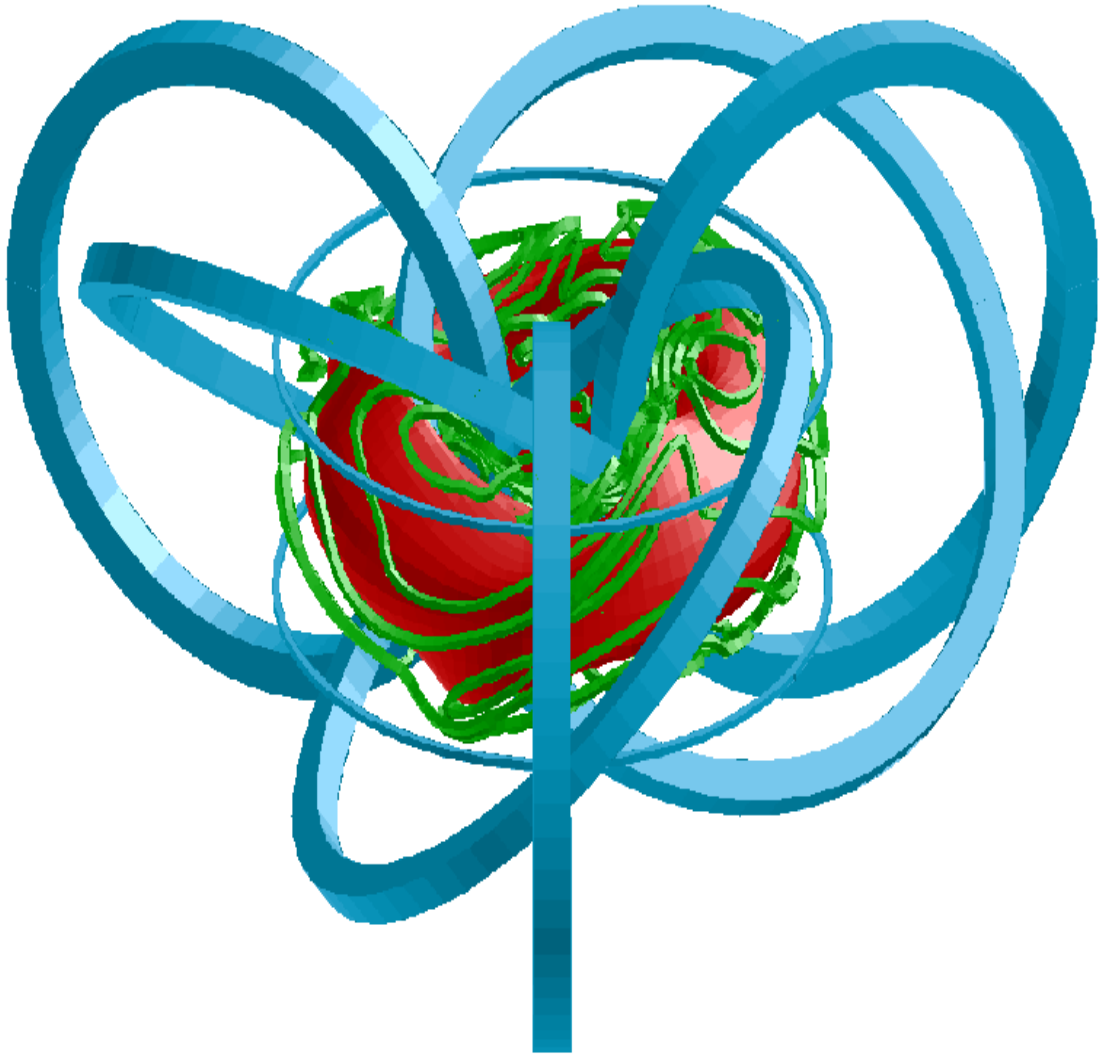

Figure 6: L=3 coil option with saddle coils. The option features 3 circular tilted, interlocking coils that enclose the major axis and the plasma (L=3 coils), 3 circular (vertical) TF coils, and 1 pair of circular PF coils for equilibrium control. Background coils are shown in blue; Saddles are shown in green.

The main problems with engineering this L=3 option are
(a) restricted access for neutral beams on the outboard midplane, and
(b) very large stray fields in the vicinity of the neutral beams.

Modular coils were also considered (see Fig. 7). Reductions in current density of about 50% have been achieved, and stray fields are not of concern for the neutral beams. There are, as yet, a number of unresolved issues relating to coil fabrication, assembly, support and alignment.

5. Modular Coil Design: COILOPT[8]

A new coil optimization code, COILOPT, has been successfully applied to the design of modular coils for compact stellarators. It uses simple 1- and 2-D fourier representations for the coil winding law and toroidal winding surface:

Winding surface:

$$R = \sum R_{mn} \cos(m\theta + n\phi), Z = \sum Z_{mn} \sin(m\theta + n\phi). \quad (3)$$

Coil winding law:

$$\phi(\theta) = \phi_0 + \sum_k [a_k \cos(k\theta) + b_k sin(k\theta)]. \quad (4)$$

The coilset depends on, typically, ~ 100 independent parameters, much less than representations that use filament segments to represent the coils. This leads to a fast design code.

A Levenberg-Marquandt optimization scheme targets B_{err}^{rms}. Plasma-coil and coil-coil separations are used to control current density; coil curvature and length are used to constrain variation of the winding surface.

Allowing the CWS to vary is crucial to the success of COILOPT. Fig. 7 shows resulting modular design.

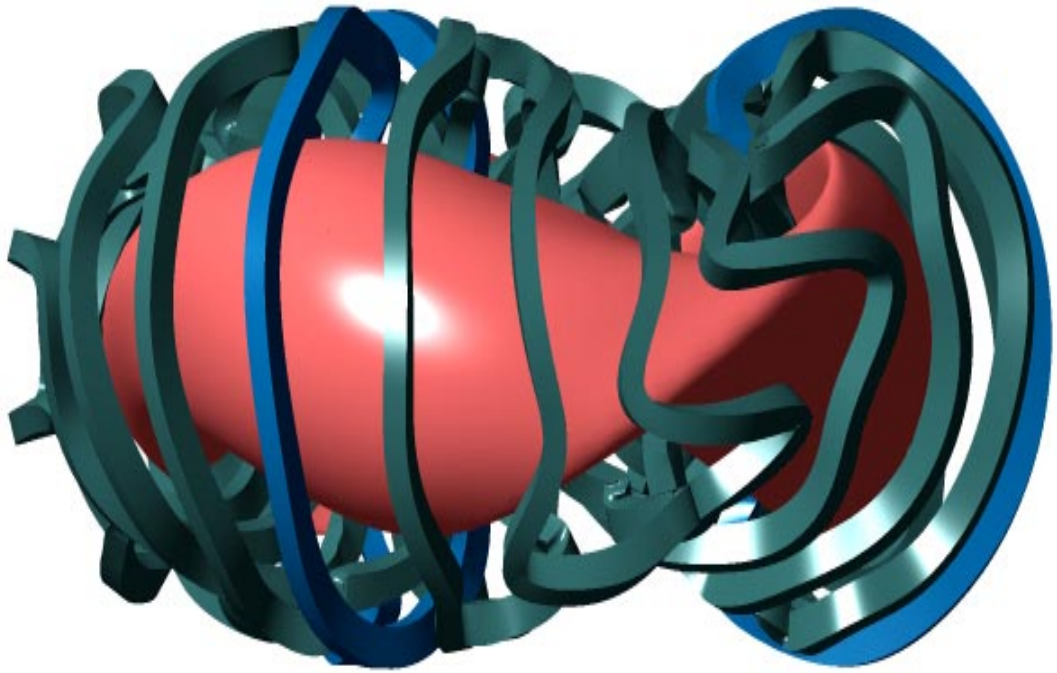

Figure 7: Modular coils for NCSX-LI383 obtained using COILOPT. There are seven coils/period and four unique coils. The current density in the copper is $12kA/cm^2$. Physics properties of the reconstructed plasma are acceptably close to the original fixed boundary configuration.

6. Integrated Coil-Plasma Design

Traditional methodology for coil-plasma system design is two-stage:

(1) Identify an attractive plasma configuration.

(2) Seek coils which match $\vec{B} \cdot \hat{n}$ on the plasma surface.

Given the coils, test engineering figures of merit (eg I_c^{max}, coil curvature). If unsatisfactory, change the plasma configuration and repeat the process.

Presently, we incorporate some engineering constraints into plasma configuration design (eg call NESCOIL within configuration optimizer, assigning a penalty to configurations with high coil complexity[11] and current density).

We are developing additional strategies which penalize configurations which require short wavelength magnetic fields, since such fields can be problematic for plasma control.

The new strategies make use of "natural functions" [10].

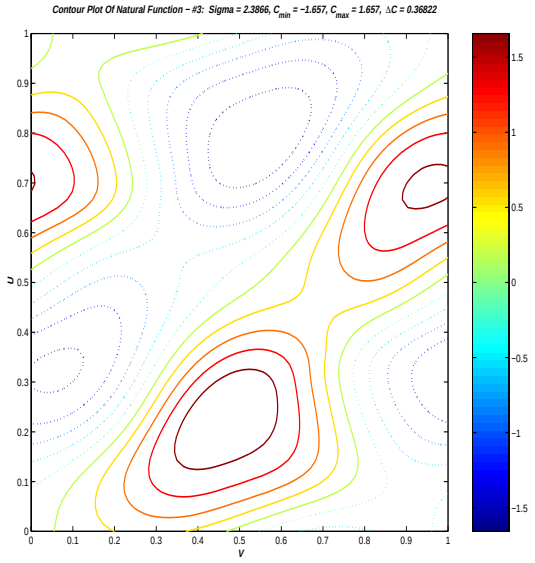

Figures 8: Contours of natural function $f_3(u, v)$ for conformal CWS with 18 cm normal separation from LI383 plasma boundary. The f_i are eigenfunctions of a Helmholtz operator whose matrix elements depend only on the geometry of the CWS. In the limit of infinite aspect ratio and a cylinder, the eigenvector shown corresponds to $m = 1, n = 1$. Below is shown the equivalent NESCOIL sine basis function.

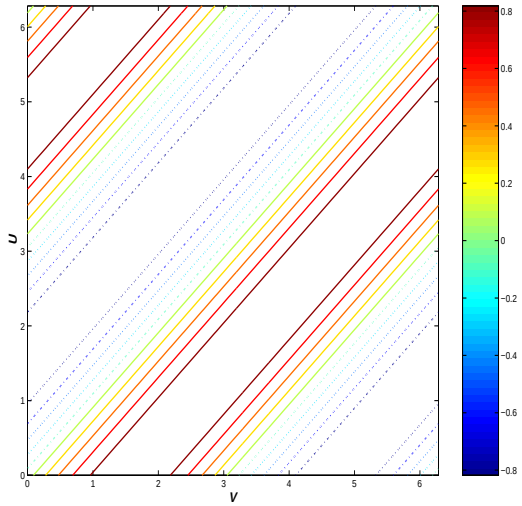

"Natural Functions" are a complete set of functions on a surface with special properties that should be useful in coil design: Each natural function, $f_i(u, v)$, describes a smooth distribution of current, and is labelled by an eigenvalue that measures how rapidly its associated magnetic field decreases with distance from the current source.

NESCOIL represents distributions of current on a CWS using fourier sine functions. The $f_i(u, v)$ are an alternative representation for the current, that suggest the following integrated plasma-coil design strategy:

Choose a CWS and determine the lowest $N_f \sim 50$, say, natural functions $f_i(u, v)$.

In a free-boundary optimizer,vary N_f coefficients, c_i in the current potential $\Phi(u, v) = \sum_i c_i f_i(u, v)$ (cf., Eq 1), to minimize physics (and possibly other engineering) penalty functions.

Alternatively, in a fixed-boundary optimizer, as the plasma shape is varied, associate a penalty representing the failure to fit $\vec{B} \cdot \hat{n}$ with the lowest N_f natural functions.

These strategies are currently under development.

Acknowledgements and References

We would particularly like to thank Peter Merkel and Michael Drevlak for use of NESCOIL and ONSET and for their support of our design efforts. This work was supported by US Department of Energy Contracts Nos. DE-AC020-76-CHO3073, DE-FG02-95ER54333, DE-FG03-95ER54296 and DE-AC05-00OR22725.

[1] VALANJU, P., et al., "Stellarator Coil Design using Enhanced Green's Function Techniques" (in preparation).
[2] MERKEL, P., Nucl. Fusion **27** (1987) 867.
[3] PRESS, W.H., et al., "Numerical Recipes" (Cambridge University Press, 1996), p.51ff
[4] MYNICK, H., POMPHREY, N., "Control Matrix Approach to Stellarator Design and Control" (to appear in Phys. Plasmas).
[5] NEILSON, G.H., et al., "Physics issues in the design of high-beta, low-aspect-ratio stellarator experiments" Phys. Plasmas **7** (2000) 1911.
[6] MINER, W.H., et al., "Use of a Genetic Algorithm for Compact Stellarator Coil Design" (submitted to Nuclear Fusion, Oct 2000)
[7] GOLDBERG, D.E., "Genetic Algorithms in Search, Optimization, and Machine Learning", (Addison Wesley, New York) 1989.
[8] STRICKLER, D.J., BERRY L.A., HIRSHMAN, S.P., "Optimization of Modular Coils for Compact Stellarators" (in preparation)
[9] DREVLAK, M., Fusion Technology **33** (1998) 106.
[10] BOOZER, A.H., "Stellarator Coil Optimization by Targeting the Plasma Configuration", Phys. Plasmas **7** (2000) 3378.
[11] HIRSHMAN, S.P., Private Communication